Journal of Metals, Materials and Minerals, Vol. 33, No. 2, pp. 148-155, 2023

Dielectric properties and electrochemical behavior of graphene oxide derived from myanmar coal minerals

Min Maung MAUNG[1,*], Chan Nyein AUNG[1], Gasidit PANOMSUWAN[2], and Khin Khin WIN[1]

[1] *University of Yangon, University Avenue Road, Yangon, 11041, Myanmar*
[2] *Kasetsart University, 50 Ngamwongwan Rd, Lat Yao, Chatuchak, Bangkok 10900, Thailand*

***Corresponding author e-mail:** minaerchan@gmail.com

Received date:
22 April 2022
Revised date
31 March 2023
Accepted date:
1 April 2023

Keywords:
Dielectric constant;
AC conductivity;
Flat-shaped capacitors;
Super capacitor

Abstract

Graphene Oxide (GO) metal nanocomposites make up an emerging class of advanced materials and enhance material functionality to obtain multifunctional properties and working towards superior performance of energy storage devices. GO was derived from Myanmar coal minerals using Modified Hummer method. The silver and nickel nanoparticles were used as metal ions or metal nanoparticles to form GO nanocomposites. Their characteristics were identified by XRD, SEM and Raman Spectroscopy. The energy gap of GO and GO composites was also investigated by the aid of UV-Vis spectroscopy. The dielectric constant is measures of the amount of electrical energy that can be stored in GO derived from coal mineral. The frequency-dependent dielectric properties and AC conductivity has been explored using GW INSTEK LCR-8110 meter. It was found that the dielectric constant is maximum at low frequencies region and decreases with increasing frequency. The electrochemical performance of this sample was examined by cyclic voltammetry (CV) measurement. The CV curves of GO have typical rectangular-like shape and no evident oxidation/reduction peak. The prototypes of flat-shaped capacitors were prepared and their capacitive values were also determined. The as-prepared GO on the copper foil can be directly used to fabricate solid-state super capacitor.

1. Introduction

Energy consumption is expanding globally on a daily basis, and existing energy supplies are insufficient to meet our energy demands. Therefore, energy depletion and environmental degradation have driven interest in discovering clean and renewable energy sources. As a result, there is an emphasis on creating an unique alternative energy source that can be stored for a longer duration [1]. Super-capacitors have attracted a lot of attention as a new type of pollution-free electrical energy storage technology with a high-power density and a long cycle life. In industries including as mobile devices and electric vehicles, they have partially replaced traditional rechargeable batteries. However, supercapacitors output less energy than batteries [2]. Many studies of material-oriented research, such as metal oxides, metal hydroxides, and two dimensional (2D) nanomaterials for energy-related applications, have recently been published [3-5]. Among them, carbon nanomaterials, such as graphene and carbon nanotubes, have developed as supercapacitor electrode materials [6]. Graphene is a 2D single-atom carbon sheet that is only one atom thick [7]. Since, it has unique electrical properties, it has gained increasing attention in recent years [8] and offers significant promise for super-capacitor electrodes [9].

In the past decades, many researchers have investigated the use of numerous noble metals like ruthenium (Ru), palladium (Pd), rhodium (Rh), silver (Ag), gold (Au), platinum (Pt), nickel (Ni) and others as electrode materials [10-12]. Noble metals can improve supercapacitance by providing efficient electron transport routes during charging and discharging cycles, but their high cost and rarity limits their use as electrode materials on a massive scale. As a result, combining a noble metal with a less expensive metal can be recognized as an effective approach for synthesizing electrode materials [10]. Since Ag has the highest electrical conductivity as well as it is low cost compared with other noble metals and Ni exhibits interesting electrochemical redox reaction [12]. Therefore, in this research, we have chosen Ag and Ni noble metals and are reporting the dielectric and electrochemical properties of co-doped Ag/Ni-GO composite. Moreover, in this study, Myanmar coal is proposed to be an alternative source of graphite as raw material to prepare graphene oxide because of the second rich category (abundance) in Myanmar.

To the best of our knowledge, there is no report about the co-doping of Ag and Ni into GO derived via Myanmar Coal. In this study, GO was synthesized using famous modified hummers method, the co-doped Ag/Ni nanoparticles GO composite were fabricated by solid state method.

The structural and morphological properties of the composites were identified by X-ray diffractometry (XRD), Raman spectroscopy and Scanning electron microscopy (SEM) techniques. The conductivity and dielectric behaviours were also determined using an LCR meter and the electrochemical characteristics was carried out by cyclic voltammetry equipment. The prototype of double layer flat-shaped capacitor was prepared and their capacitance values were also investigated.

2. Materials and methods

2.1 Materials

Potassium Permanganate ($KMnO_4$), Sulphuric acid (H_2SO_4), Hydrochloric acid (HCl), Hydrogen peroxide, Sodium Nitrate ($NaNO_3$), and Deionised water (DI) were purchased from Sigma Aldrich, Singapore. The coal powder was naturally occurring and collected from the Kalaywa region, Upper Myanmar. Nickel (II) Nitrate hexahydrate ($Ni(NO_3)_2$-$6H_2O$, Silver Nitrate ($AgNO_3$), Polyvinyl-pyrrolidone (PVP) and Sodium hydroxide were purchased from Thermo Fisher Scientific, Singapore.

2.2 Preparation of GO fine powder

In experimental procedure, graphene oxide (GO) was synthesized using famous modified hummers method from naturally occurred coal powder. The coal power was grounded by using PBL-LS-1 ball machine with 37 rpm to 370 rpm and 30 min. The power was used without any further purification. In this method, 1.2 g of coal powder and 2 g of sodium nitrate were taken in a beaker containing 50 mL of concentrated sulphuric acid (H_2SO_4). The reaction mixture was stirred for 2 h in ice-cold water to maintain its temperature 0°C to 6°C, and then 6 g of $KMnO_4$ was slowly added to the reaction mixture for continuous stirring of 2 h. The sample mixture was stirred at 30°C until it turns into a brownish paste and continued stirring for another 2 h. The reaction was weakened with the addition of 100 mL of DI water and the solution mixture was finally treated with 8 mL of H_2O_2 to terminate the reaction [13,14]. Finally, the mixture was centrifuged and rinsed with 8% HCl followed by DI water for five times. The obtained precipitates were filtered, dried, and grounded in fine powder form for further purpose.

2.3 Synthesis of Silver Nanoparticles (AgNPs)

Firstly, the AgNPs were prepared by chemical reduction of an aqueous solution 1 M of $AgNO_3$. 1 g of Polyvinylpyrrolidone (PVP) was dissolved in 60 mL of 0.45 M NaOH solution and heated 2°C·min^{-1} to 60°C for continuous stirring of about 45 min. Secondly, 20 mL of AgNPs solution was added to the PVP solution by drop method and stirred for about 10 min [15,16]. Finally, the mixture solution was centrifuged, filtered, washed in distilled water and dried at room temperature for 24 h [17].

2.4 Synthesis of nickel nanoparticles (NiNPs)

Nickel (II) nitrate hexahydrate $Ni(NO_3)_2 \cdot 6H_2O$ (0.02 mol) was dissolved in 10 cm^3 distilled water and mixed together with 10 cm^3 of benzildiethylenetriamine (0.004 mol). After being stirred and refluxed for 2 h at moderate temperature, the colour of the solution became pale blue to black. Finally, the mixture was centrifuged, filtered, washed with acetone and dried at room temperature for 24 h [18,19].

2.5 Synthesis of GO-Ag and GO-Ni Nanocomposites

GO powder and AgNPs with the ratio of 2:1 was mixed and taken in 50 mL of methanol. The mixture was sonicated for 2 days followed by thermal annealing at 400°C. Then, keep subsequent cold freezing. The process of sonication, annealing and cold freezing were done twice. The dried and homogenized GO-Ag powder was obtained. Similarly GO-Ni nanocomposite was also prepared as the process of GO-Ag nanocomposite [20,21].

2.6 Measurements and Data Acquisition

The phase and structure improvement were studied by Rigaku SmartLab, X-ray powder diffraction (XRD) with scanning rate of 50.00°C·min^{-1} and generating 20 kV and 10 mA. The scan range of 5~80° and CuK_β window was used for these measurements. Scanning Electron Microscope (SEM) was used for studying of surface morphologies and roughness. In this work, we used JEOL-JSM 5610 LV with 15 KV, sport size 20 and working distance 10 mm. Shimadzu UV-1800 Spectrophotometer was used for absorption studies in the range of 200-800 nm under the absorption mode.

3. Results and discussion

3.1 XRD Analysis

In this analysis, XRD was used to study the crystal structure and verify the inter layer spacing of GO, GO-Ag and GO-Ni nano-composites. Figure 1 shows the XRD pattern of synthesized GO, GO-Ag and GO-Ni nnanocomposites. The XRD pattern of GO exhibits a strong at the angle of $2\theta = 10.19°$ value that corresponds to the plane (001)[22]. Additionally, a small peak at $2\theta = 54.93°$ was observed, which reflects the (002) plane. It means some residual graphite was observed in the GO composites [23]. In GO, the interlayer spacing increased as compared to graphite due to addition of oxygen-containing functional groups during oxidation of graphite [24,25]. The GO-Ag and GO-Ni nanocomposites exhibited a peak related to GO, Ag nano-particle and Ni nanoparticle respectively. In XRD pattern of GO-Ag, the intensity peaks show at 38.5°, 45.4°, 65.2° and 77.6°, corresponding to Ag phase (111), (200), (220) and (311) which are corresponding to Ag doped GO composites [21] and well match with the PDF 03-065-1528. The GO-Ni nanocomposites show the major diffraction peaks at 45.2°, 52.4° and 76.5° which are corresponding to the Ni phase (111), (200) and (222) [26].

3.2 Raman spectroscopy measurement

Raman spectroscopy was used to analyse structural features of graphene oxide. The Raman spectra of GO, GO-Ag and GO-Ni were shown in Figure 2. In this spectra, the G band corresponds to sp^2 hybridised carbon-based material and D peak is related to defect or lattice disorder due to the binding of oxygen-functional group [27]. The intensity of the D band is associated with the size of the sp^2 in-plane domains. The I_D/I_G ratio (calculated from the intensity of D and G bands) can be used to characterise the disorder of the graphitic structure in carbon materials [28,29]. From Figure 2, it was found that GO exhibited D at 1362.42 cm^{-1} attributed to the structural defect (partially disordered) of the aromatic (conjugation) carbon-carbon bonds and G bands at 1563.79 cm^{-1} due to the sp^2 carbon bond stretching reveals the lattice distortions. Another peak 2D band (defect activated peaks) was also appeared at 2878.07 cm^{-1}. The I_D/I_G ratio of GO

was obtained 0.87. The D and G bands of the GO-Ag nanocomposite and GO-Ni nanocomposite appeared at 1353.12, 1355.32 and 1592.64, 1600.29 cm^{-1}, respectively [30]. It can be seen that there was no significant changes in the Raman shifts of the D-band and G-band, but there is a significant difference in the I_D/I_G value. The D band was assigned to the breathing mode of k-point phonons with A_{1g} symmetry, and the G band was ascribed to E_{2g} phonon of sp^2 carbon atoms. After doping, the D and G band values increase due to intercalation of AgNPs, and NiNPs on the GO surface [31]. Based on the Raman spectra, the I_D/I_G ratios were calculated as 0.84 and 0.85 for GO-Ag and GO-Ni, respectively. The intensity ratios of these bands help to estimate the defect in the sample, whereby GO presents more defects compared to GO-Ag and GO-Ni nanocomposites. The I_D/I_G ratio of these two samples is less than that of GO sample and it indicates that the degree of graphitization of these samples was enhanced [32].

3.3 SEM analysis

The coal minerals from Kalaywa region, Myanmar is medium-grade coal with carbon content of 85%. It has some impurities and is porous with a primary porosity of macropores. The surface morphology and layer structure of GO, GO-Ag and GO-Ni nanocomposites were examined by SEM spectroscopy. The Figure 2 shows the formation of graphene oxide with a closely packed lamellar structure and a well packed layered structure [33]. Although it has some impurities which does not show the proper multilayered structure and is instead in the form of flakes[34]. The porous stacking structures of graphene oxide were observed in GO sample and many pores that appear in the stacked structure in GO-Ag and GO-Ni nanocomposites. It was observed that many white spots include in GO-Ag sample which indicates that silver nanoparticles were uniformly spread around and not only on the surface of the composites. The significant aggregation of the Ni nanoparticles was interacted with GO and inhibit their aggregation after incorporation of them into composite materials. Since the charge is stored throughout the bulk of the materials, the porous structure and the functional groups together can be increased the capacitance effect at the electrode/electrolyte interface [35,36].

3.4 UV-Vis analysis

The absorption spectra of the GO, GO-Ag and GO-Ni exhibited strong, broad peaks at 226, 236, 414, 238 and 434 nm, respectively are shown in Figure 3(a). The UV-vis absorption spectrum of the GO sample shows a characteristic band at 226 nm, which corresponds to the electronic π–π* transitions of C–C aromatic bonds, and a shoulder at 300 nm, which can be assigned to the n–π* transitions of C=O bonds. GO-Ag nanocomposites exhibited absorption band at 236 nm and 414 nm, indicating the presence of Ag in the GO dispersion and GO-Ni nanocomposites also exhibited absorbance bands at 238 nm and 434 nm. The presence of a band at 414 nm in the GO-Ag dispersion is attributed to the surface resonance of silver nanoparticles in the composite and a band 434 nm in the GO-Ni is attributed to the surface resonance of nickel nanoparticles in this composite [35,37].

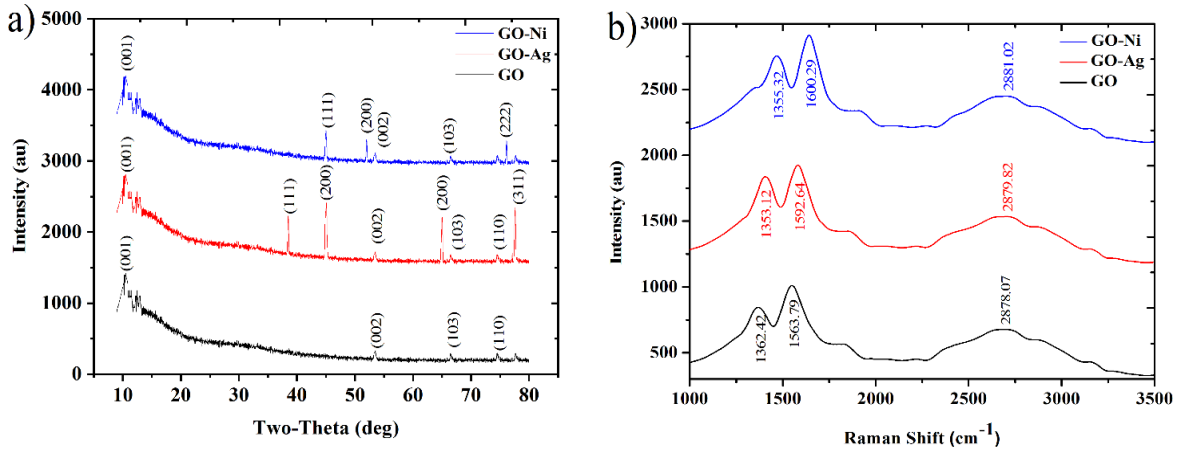

Figure 1. Spectra of nanocomposites (a)XRD spectra of GO, GO-Ag and GO-Ni (b) Raman spectra of GO, GO-Ag and GO-Ni nanocomposites.

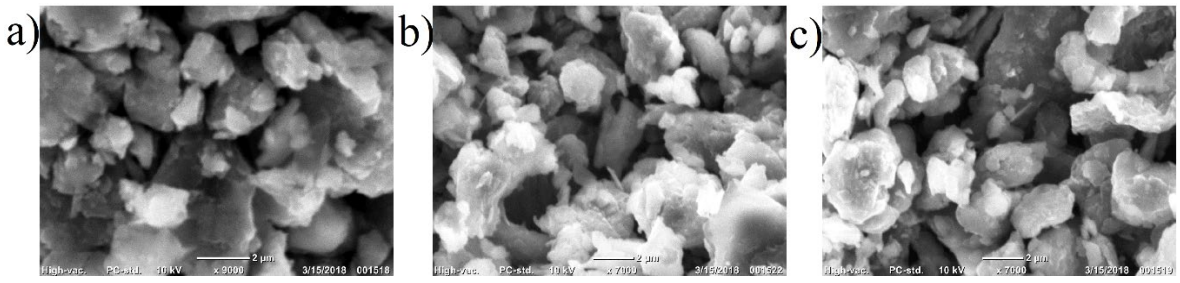

Figure 2. The SEM images (a) GO, (b) GO-Ag and (c) GO-Ni nanocomposites.

3.5 Dielectric properties of GO, GO-Ag and GO-Ni nanocomposites

Dielectric properties of synthesized graphene oxide (GO), GO-Ag and GO-Ni nanocomposites have been studied in the frequency range of 1-10^6 Hz. The dielectric constant decreases with increasing frequency was shown in Figure 3(b-c). It was due to orientation of charges and rotation of dipoles moment of functional group present on the graphene oxide [38]. It was also observed that the dielectric constant increases with temperature due to highly conductive nature of graphene oxide and GO nanocomposite samples. Electrical conductivity of graphene oxide increases exponentially with increasing frequency was shown in Figure 3(d). Electrical conductivity and dielectric permittivity increases with temperature due to thermal activation of charge carriers and positive temperature coefficient effect of conductance [39].

3.6 Cyclic voltammetry measurement

The obtained GO, GO-Ag and GO-Ni nanocomposites were used as an electrode material for supercapacitor application. In a typical electrochemical measurement, aqueous solution of 0.1 M NaCl was used as electrolyte. The specific capacitance was calculated by using the equation: $C_s = \frac{\int I\, dV}{m\, v\, \Delta V}$ = where C_s = Specific capacitance (F·g^{-1}), $\int I\, dV$ = are under CV curve, m = mass of active material (g), v = potential scan rate (mV/s), ΔV = potential window (V).

CV graphs of GO show a cathodic peak potential at 0.04 V and an anodic peak potential at -0.6 V because of the presence of favourable oxygenated species on the GO surface, which create edge plane defects during the electrochemical reaction. It has been noted that oxygenated species can alter the observed electrochemistry of this redox probe [40]. The CV curves of GO have typical rectangular-like shape and no evident oxidation/reduction peak because it contains the more functional group. GO has excellent behaviors of electrochemical double-layer capacitance, and also reflects a highly reversible and reliable electrosorption charge-discharge process. The CV hysteresis area is related to the current response of GO electrode, which at the higher scan rates the GO electrode can give the higher current response [41].

For all potential windows, the specific capacitance of GO is higher at lower scan rate which is attributed to the more ion diffusion into the micro and mesopore surface of GO (enough time for ion diffusion at low scan rate). Due to the internal resistance of the electrode, the shape is slightly distorted from rectangular and close to parallelogram, indicating that the main contribution to the capacitance is the charge and discharge of the double layer. The presence of various functional groups in the materials contributes in the form of pseudo capacitance, as can be seen from the anodic and corresponding cathodic peaks, from the redox reaction of surface functional groups. The increase in the current density with increase in level of oxidation can also be visualized from the CV profiles [42]. The capacitance decreases at higher scan rates for all the samples and also there exists lot of distortion in the CV spectrum. The distortion in the CV and the decreased capacitance at higher scan rates are mainly due to the increase in the inaccessible sites within the electrode [36].

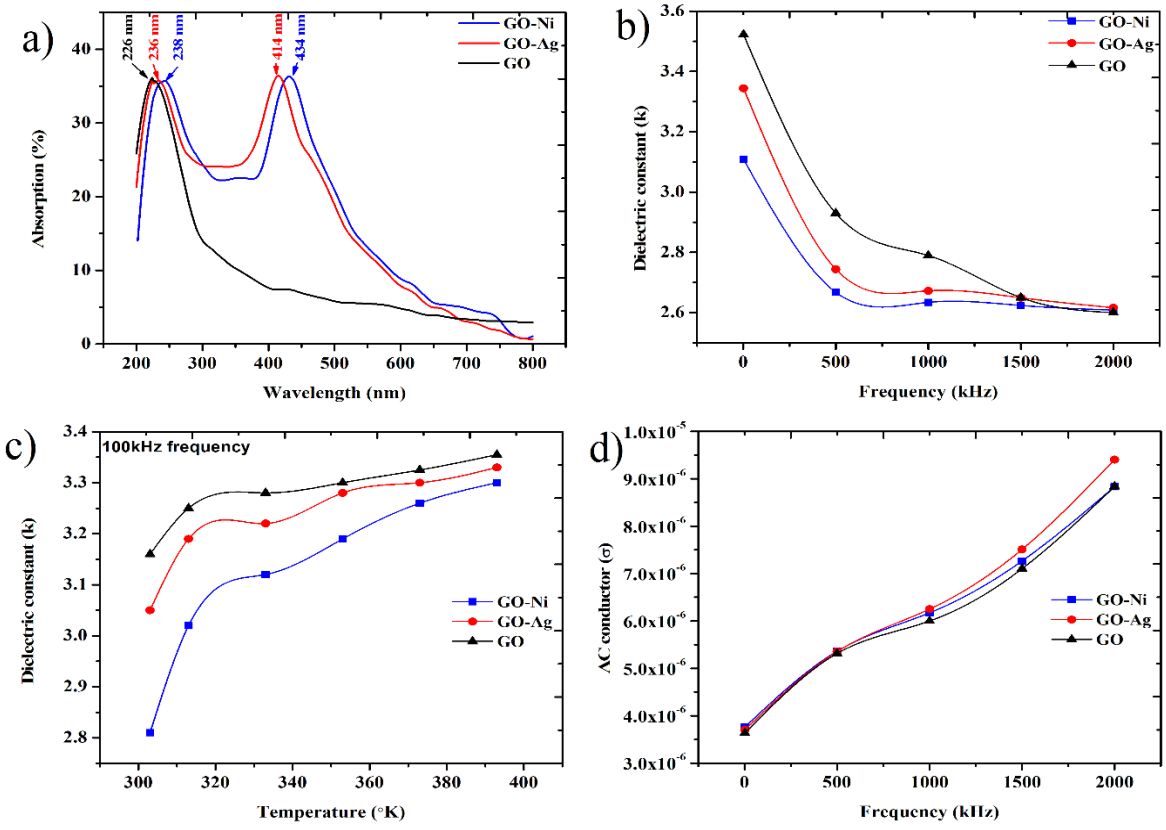

Figure 3. UV-Vis absorption and electrical properties of GO,GO-Ag and GO-Ni composities (a) Absorption graph (b) Dielectric constant (**k**) vs frequency (c) Dielectric constant (**k**) and temperature(˚K) (d) AC conductor (a) vs frequency.

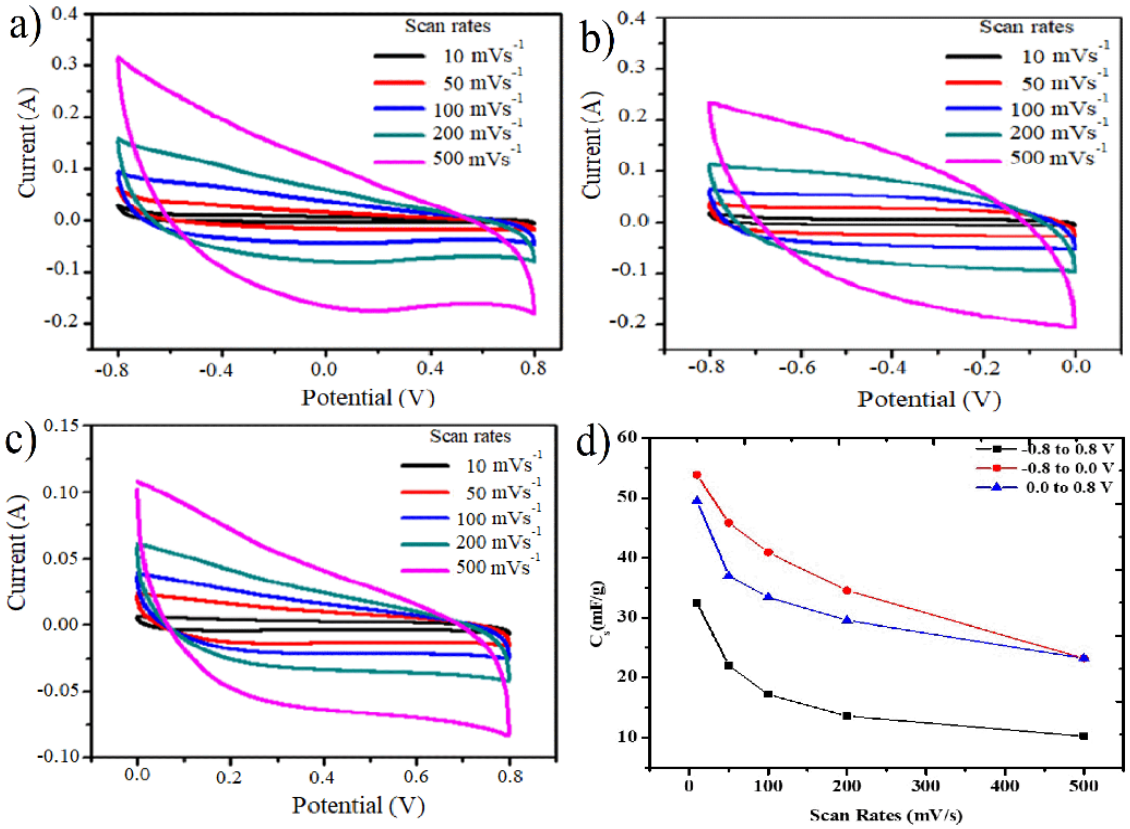

Figure 4. The CV plot of graphene oxide with different potential windows (a) Current vs potential graph for (-0.8 to 0.8V) (b) Current vs potential graph for (-0.8 to 0.0V) (c) Current vs potential graph for (0.0-0.8V), and (d) The calculated specific capacitance

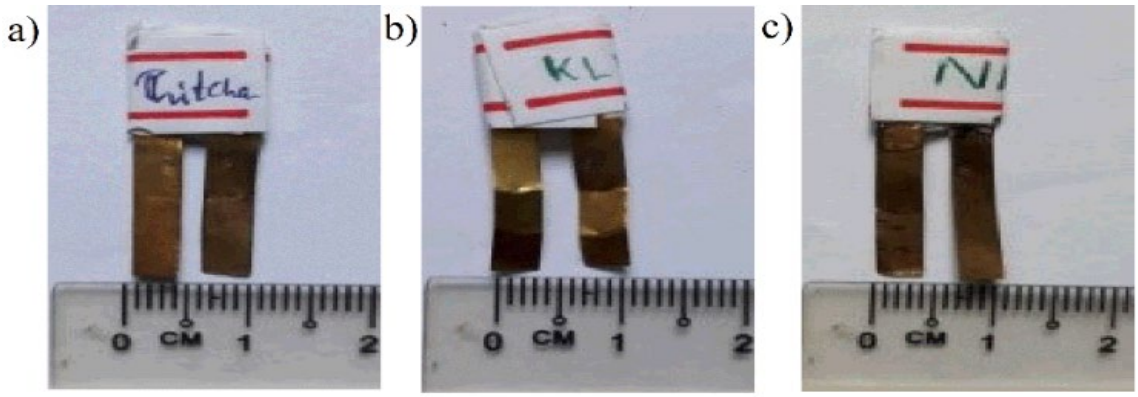

Figure 5. The photographs of the prototype flat-shaped capacitors with the area of 1 cm^2 using a) GO, b) GO-Ag and c) GO-Ni.

3.7 Double layer flat-shaped capacitor

Three size of prototypes flat-shaped capacitors (1 cm^2, 4 cm^2 and 6 cm^2) were prepared with GO, GO-Ag and GO-Ni nanocomposite electrodes. Polyvinyl alcohol (PVA) was used as agent solution in preparation of these prototypes capacitor. 1 g of polyvinyl alcohol (PVA) was stirred to dissolve in 100 mL distilled water at 100°C for 30 min. Then, the solution was cooled down in room temperature. 1 g of GO powder was added in this solution to make the suitable adhesive form. The obtained sample was incrusted uniformly on the thin copper foil. It was slowly dried in the room temperature. The separator between two electrodes was used tissue paper to control ion exchange among their electrodes [43]. The prototype flat-shaped capacitors were shown in Figure 5.

The measured value of capacitance was shown in Table 1 and the equivalent series resistance (ESR) was calculated by the equation ESR = D/2πfC. It was found that the higher capacitance value of capacitor, it was the smaller of ESR value. The calculated value of ESR of each capacitor was shown in Table 2. The capacitance-voltage (CV) characteristics of each capacitor electrode with different surface areas were also determined [44,45].

The high conductive noble metal Ag and Ni create space between the graphene nanosheets resisting the restacking graphene layers, which enhance the conductivity of the material and the diffusivity of electrolyte and increase the effective exposer area of the graphene layers. Thus, these GO nanocomposites achieved a high energy density and showed excellent long cyclic stability.

Table 1. The capacitance of each sample with different area.

Samples	Capacitance (μF)		
	1 cm^2 size	**4 cm^2 size**	**6 cm^2 size**
GO	31.93	132.24	295.42
GO-Ag	45.61	170.49	305.04
GO-Ni	64.77	206.24	407.63

Table 2. The calculated value of ESR of each capacitor.

Samples	Equivalent Series Resistance (ESR) (Ω)		
	1 cm^2 size	**4 cm^2 size**	**6 cm^2 size**
GO	1.711	0.318	0.015
GO-Ag	0.191	0.143	0.014
GO-Ni	0.134	0.017	0.011

4. Conclusion

Myanmar coal is used to be an alternative source of graphite as raw material to prepare graphene oxide. Inherently, coal has the disordered configuration and small crystalline domains. This is the advantages of coal to extract the graphene oxide because of easy dispersion, exfoliation, functionalization and chemical cutting [46]. Graphene oxide was synthesized by Modified Hummers method and GO-Ag and GO-Ni nanocomposites were synthesized by chemical reduction method respectively. The characteristics peaks (001) at 10.19° for GO can be detected from XRD result. The microstructural information about conjugated and carbon-carbon bonds of synthesized samples was determined and their I_D/I_G ratio was also calculated. It was indicated that GO sample presents more defects compared to GO-Ag and GO-Ni nanocomposites and the degree of graphitization of these two nanocomposite samples was enhanced [47]. SEM image depicted that aggregated and crumpled structures were found in all samples and the macro porous structure of these samples can be increased their capacitance effect. UV-Vis spectrum of GO exhibits maximum absorption peak at 226 nm corresponding to a π-π* transition of the aromatic C=O bonds from oxidized of graphite oxide solution. Dielectric constant decreases with frequency due to orientation of charges and rotation of dipoles, and increases with temperature due to highly conductive nature of graphene oxide nanoparticles. The CV measurements for all potential windows, the Cs is as high as 54 $mF \cdot g^{-1}$ at low scan rate of 10 $mV \cdot s^{-1}$ which is attributed to the more ion diffusion into the micro and mesopore surface of GO (enough time for ion diffusion at low scan rate) [48]. Comparative studies of GO and GO-Ag nanocomposite will provide insight into the doping of metal nanoparticles in the graphene oxide moiety to enhance its practicability in electrode materials.

Acknowledgements

The authors gratefully acknowledge the financial supports by the ICE-Matter Project (CR-2020).

References

[1] A. R. Ansari, S. A. Ansari, N. Parveen, M. O. Ansari, and Z. Osman, "Silver nanoparticle decorated on reduced graphene oxide-wrapped manganese oxide nanorods as electrode materials for high-performance electrochemical devices," *Crystals*, vol. 12, no. 3, 2022.

[2] J. Hong, S. J. Park, and S. Kim, "Synthesis and electrochemical characterization of nanostructured Ni-Co-MOF/graphene oxide composites as capacitor electrodes," *Electrochimica Acta*, vol. 311, pp. 62-71, 2019.

[3] T. M. Gür, "Review of electrical energy storage technologies, materials and systems: Challenges and prospects for large-scale grid storage," *Energy and Environmental Science*, vol. 11, no. 10. pp. 2696-2767, 2018.

[4] J. Kim, S. C. Byun, S. Chung, and S. Kim, "Preparation and capacitance properties of graphene based composite electrodes containing various inorganic metal oxides," *Carbon Letters*, vol. 25, no. 1. pp. 14-24, 2018.

[5] A. H. Khan, S. Ghosh, B. Pradhan, A. Dalui, L. K. Shrestha, S. Acharya, and K. Ariga "Two-dimensional (2D) nanomaterials towards electrochemical nanoarchitectonics in energy-related applications," *Bulletin of the Chemical Society of Japan*, vol. 90, no. 6, pp. 627-648, 2017.

[6] S. Xiong, Y. Shi, J. Chu, M. Gong, B. Wu, and X. Wang, "Preparation of high-performance covalently bonded polyaniline nanorods/graphene supercapacitor electrode materials using interfacial copolymerization approach," *Electrochimica Acta*, vol. 127, pp. 139-145, 2014.

[7] A. K. Geim, and K. S. Novoselov, "The rise of graphene," in Nanoscience and Technology: A Collection of Reviews from Nature Journals, 2009, pp. 11-19, 2009.

[8] K. S. Novoselov, A. K. Geim, S. V. Morozov, D. Jiang, S. V. Dubonos, I. V. Grigorieva, and A. A. Firsov, "Electric field effect in atomically thin carbon films," *Science*, vol. 306, no. 5696, pp. 666-669, 2016.

[9] J. Abraham, K. S. Vasu, C. D. Williams, K. Gopinadhan, Y. Su, C. T. Cherian, J. Dix, E. Prestat, S. J. Haigh, I. V. Grigorieva, P. Carbone, A. K. Geim, and R. R. Nair, "Tunable sieving of ions using graphene oxide membranes," *Nature Nanotechnology*, vol. 12, no. 6, pp. 546-550, 2017.

[10] Y. Yan, T. Wang, X. Li, H. Pang, H. X.-I. C. Frontiers, and U. "Noble metal-based materials in high-performance super-capacitors," *Royal Society of Chemistry (pubs.rsc.org),* vol. 4, no. 1, pp. 33-51, 2017.

[11] S. Khamlich, T. Khamliche, M. S. Dhlamini, M. Khenfouch, B. M. Mothudi, and M. Maaza, "Rapid microwave-assisted growth of silver nanoparticles on 3D graphene networks for supercapacitor application," *Journal of Colloid Interface Science*, vol. 493, pp. 130-137, 2017.

[12] M. Chandel, P. Makkar, and N. N. Ghosh, "Ag-Ni nanoparticle anchored reduced graphene oxide nanocomposite as advanced electrode material for supercapacitor application," *ACS Applied Electronic Materials*, vol. 1, no. 7, pp. 1215-1224, 2019.

[13] N. I. Zaaba, K. L. Foo, U. Hashim, S. J. Tan, W. W. Liu, and C. H. Voon, "Synthesis of graphene oxide using modified hummers method: Solvent influence," *Procedia Engineering*, vol. 184, pp. 469-477, 2017.

[14] S. N. Alam, N. Sharma, and L. Kumar, "Synthesis of graphene oxide (GO) by modified hummers method and its thermal reduction to obtain reduced graphene oxide (rGO)*," *Graphene*, vol. 06, no. 01, pp. 1-18, 2017.

[15] H. Wang, X. Qiao, J. Chen, and S. Ding, "Preparation of silver nanoparticles by chemical reduction method," *Colloids Surfaces A: Physicochemical and Engineering Aspects*, vol. 256, no. 2-3, pp. 111-115, 2005.

[16] E. C. Gloria, E. Velez, M. Gladis, H. Cesar, J. Osorio, O. Arnache, J. I. U. Alzate, and F. Jaramillo, "Synthesis of silver nanoparticles (AgNPs) with antibacterial activity," *Journal of Physics: Conference Series (JPCS)*, vol. 850, no. 1, p. 012023, 2017.

[17] S. Iravani, H. Korbekandi, S. V Mirmohammadi, and B. Zolfaghari, "Synthesis of silver nanoparticles: chemical, physical and biological methods." *Research in Pharmaceutical Sciences*," vol. 9, no. 6, pp. 385-406, 2014.

[18] R. G. Chaudhary, J. A. Tanna, N. V. Gandhare, A. R. Rai, and H. D. Juneja, "Synthesis of nickel nanoparticles: Microscopic investigation, an efficient catalyst and effective antibacterial activity," *Advanced Materials Letters*, vol. 6, no. 11, pp. 990-998, 2015.

[19] S. Chandra, A. Kumar, and P. K. Tomar, "Synthesis of Ni nanoparticles and their characterizations," *Journal of Saudi Chemical Society*, vol. 18, no. 5, pp. 437-442, 2014.

[20] L. Ma, Z. Zhu, M. Su, L. Ma, D. Liu, and Z. Wang, "Preparation of graphene oxide-silver nanoparticle nanohybrids with highly antibacterial capability," *Talanta*, vol. 117, no. December, pp. 449-455, 2013.

[21] S. Kumari, P. Sharma, S. Yadav, J. Kumar, A. Vij, P. Rawat, S. Kumar, C. Sinha, J. Bhattachary, C. M. Srivastave, and S. Majumder, "A novel synthesis of the graphene oxide-silver (GO-Ag) nanocomposite for unique physiochemical applications," *ACS Omega*, vol. 5, no. 10, pp. 5041-5047, 2020.

[22] L. Shahriary, and A. A. Athawale, "Graphene oxide synthesized by using modified hummers approach," *International Journal of Renewable Energy and Environmental Engineerring*, vol. 02, no. 01, pp. 58-63, 2014.

[23] N. M. S. Hidayah, W. W. Liu, C. W. Lai, N. N. Zulkepli, C-S. Khe, U. Hashim, and J. C. Lee, "Comparison on graphite, graphene oxide and reduced graphene oxide: Synthesis and characterization," *AIP Conference Proceedings*, vol. 1892, no. 1, p. 150002, 2017.

[24] B. Gupta, N. Kumar, K. Panda, V. Kanan, S. Joshi, and I. Visoly-Fisher, "Role of oxygen functional groups in reduced graphene oxide for lubrication," *Scientific Reports*, vol. 7, pp. 1-14, 2017.

[25] L. Luo, T. Peng, M. Yuan, H. Sun, S. Dai, and L. Wang, "Preparation of graphite oxide containing different oxygen-containing functional groups and the study of ammonia gas sensitivity," *Sensors (Switzerland)*, vol. 18, no. 11, 2018.

[26] M. M. Almutairi, E. E. Ebraheim, M. S. Mahmoud, M. S. Atrees, M. E. M. Ali, and Y. M. Khawassek, "Nanocomposite of TiO_2 @ Ni- or co-doped graphene oxide for efficient photo-catalytic water splitting," *Egyptian Journal of Chemistry*, vol. 62, no. 9, pp. 1649-1658, 2019.

[27] S. Perumbilavil, P. Sankar, T. Priya Rose, and R. Philip, "White light Z-scan measurements of ultrafast optical nonlinearity in reduced graphene oxide nanosheets in the 400-700 nm region," *Applied Physics Letter*, vol. 107, no. 5, pp. 10-15, 2015.

[28] P. Puech, M. Kandara, G. Paredes, L. Moulin, E. Weiss-Hortala, A. Kundu, N. Ratel-Ramond, J-M. Plewa, R. Pellenq, and M. Monthioux, "Analyzing the raman spectra of graphenic carbon materials from kerogens to nanotubes: What type of information can be extracted from defect bands?," C — *Journal of Carbon Research*, vol. 5, no. 4, p. 69, 2019.

[29] M. Ali, "Raman characterization of structural properties of thermally modified nanographite," *Chemistry*, vol. Independen, p. 49, 2015.

[30] S. Gurunathan, J. Hyun Park, Y.-J. Choi, J. Woong Han, and J.-H. Kim, "Synthesis of graphene oxide-silver nanoparticle nanocomposites: An efficient novel antibacterial agent," *Current Nanoscience,* vol. 12, no. 6, pp. 762-773, 2016.

[31] A. A. K. King, B. R. Davies, N. Noorbehehesht, P. Newman, T. L Church, A. T. Harris, J. M Razal, and A. I. Minett, "A new raman metric for the characterisation of graphene oxide and its derivatives," *Scientific Reports*, vol. 6, pp. 1-6, 2016.

[32] S.-G. Kim, O.-K. Park, J. H. Lee, and B.-C. Ku, "Layer-by-layer assembled graphene oxide films and barrier properties of thermally reduced graphene oxide membranes," *Carbon Letters*, vol. 14, no. 4, pp. 247-250, 2013.

[33] H. Ahmad, F. M. Husain, and R. A. Khan, "Graphene oxide lamellar membrane with enlarged inter-layer spacing for fast preconcentration and determination of trace metal ions," *Royal Society of Chemistry Advances*, vol. 11, no. 20, pp. 11889-11899, 2021.

[34] S. Hashmi, A. Mushtaq, R. Ahmed, and Z. U. Ali, "Synthesis and characterization of reduced graphene oxide from indigenous coal: A non-burning solution," *Internation Journal of Membrance Science and Technology*, vol. 9, no. 1, pp. 1-12, 2022.

[35] A. Ilnicka, M. Skorupska, M. Szkoda, Z. Zarach, P. Kamedulski, W. Zielinski, and J. P. Lukaszewicz, "Combined effect of nitrogen-doped functional groups and porosity of porous carbons on electro-chemical performance of supercapacitors," *Scientific Reports*, vol. 11, no. 1, pp. 1-12, 2021.

[36] P. Karthika, N. Rajalakshmi, and K. S. Dhathathreyan, "Functionalized exfoliated graphene oxide as supercapacitor electrodes," *Soft Nanoscience Letter*, vol. 02, no. 04, pp. 59-66, 2012.

[37] C. S. Wei, C-h. Chia, S. Zakaria, M. K Ayob, K. L. Chee, H. N. Ming, H-m, Neoh, H. Lim, R. Jamal, and R. M. F. R. Abdul Rahman, "Antibacterial performance of Ag nanoparticles and AgGO nanocomposites prepared via rapid microwave-assisted synthesis method," *Nanoscale Research Letters*, vol. 7, no. 1, pp. 1-7, 2012.

[38] H. M. Li, C. H. Ra, G. Zhang, W. J. Yoo, K. W. Lee, and J. D. Kim, "Frequency and temperature dependence of the dielectric properties of a PCB substrate for advanced packaging applications," *Journal of the Korean Physical Society*, vol. 54, no. 3, pp. 1096-1099, 2009.

[39] C. Rayssi, S. El Kossi, J. Dhahri, and K. Khirouni, "Frequency and temperature-dependence of dielectric permittivity and electric modulus studies of the solid solution $Ca_{0.85}Er_{0.1}Ti_{1-}$: XCo_4 x $/3O_3$ ($0 \leq x \leq 0.1$)," *Royal Society of Chemistry Advances*, vol. 8, no. 31, pp. 17139-17150, 2018.

[40] W. Yuan, Y. Zhou, Y. Li, C. Li, H. Peng, J. Zhang, Z. Liu, L. Dai, and G. Shi, "The edge- and basal-plane-specific electrochemistry of a single-layer graphene sheet," *Scientific Reports*, vol. 3, no. Cvd, pp. 1-7, 2013.

[41] V. Marcelina, N. Syakir, S. Wyantuti, Y. W. Hartati, R. Hidayat, and Fitrilawati, "Characteristic of thermally reduced graphene oxide as supercapacitors electrode materials," IOP Conference Series: Materials Science and Engineering, vol. 196, no. 1, pp. 6-10, 2017

[42] D. M. Morales and M. Risch, "Seven steps to reliable cyclic voltammetry measurements for the determination of double layer capacitance," *Journal of Physics and Energy*, vol. 3, no. 3, p. 034013, 2021

[43] Y. Amaregouda, K. Kamanna, T. Gasti, and V. Kumbar, "Enhanced functional properties of biodegradable Polyvinyl alcohol/carboxymethyl cellulose (PVA/CMC) composite lms reinforced with L- alanine surface modi ed CuO nanorods," *Journal of Polymers and the Enivironment*, vol. 30, no. 6, pp. 2559-2578, 2022.

[44] F. Y. Ban, S. R. Majid, N. M. Huang, and H. N. Lim, "Graphene oxide and its electrochemical performance," *International Journal of Electrochemical Science*, vol. 7, no. 5, pp. 4345-4351, 2012.

[45] S. S. Rao, A. Stesmans, Y. Wang, and Y. Chen, "Direct ESR evidence for magnetic behavior of graphite oxide," *Physica E: Low-Dimensional System and Nanostructure*s, vol. 44, no. 6, pp. 1036-1039, 2012.

[46] R. Ye, C. Xiang, J. Lin, Z. Peng, K. Huang, Z. Yan, N. P. Cook, E. L. G. Samuel, C-C. Hwang, G. Ruan, G. Ceriotti, A-R. O. Raji, A. A. Marti, and J. M. Tour, "Coal as an abundant source of graphene quantum dots," *Nature Communications*, vol. 4, pp. 1-7, 2013.

[47] R. Sharma, N. Chadha, and P. Saini, "Determination of defect density, crystallite size and number of graphene layers in graphene analogues using X-ray diffraction and Raman spectroscopy," *Indian Journal of Pure and Applied Physics*, vol. 55, no. 9, pp. 625-629, 2017.

[48] L. L. Zhang, X. Zhao, M. D. Stoller, Y. Zhu, H. Ji, S. Murali, Y. Wu, S. Perales, B. Clevenger, and R. Ruoff, "Highly conductive and porous activated reduced graphene oxide films for high-power supercapacitors," *Nano Letters. American Chemical Society*, vol. 12, no. 4, pp. 1806-1812, 2012.